Dijkstra, J. *et al.* (2012). *Géotechnique* **62**, No. 8, 721–725 [http://dx.doi.org/10.1680/geot.8.P.124]

TECHNICAL NOTE

Electrical resistivity method for the measurement of density changes near a probe

J. DIJKSTRA*, W. BROERE* and A. F. VAN TOL*

In order to investigate changes in porosity in saturated silica sand, an electrical resistivity probe for physical model testing was developed. For non-conducting particles, electrical resistivity measurements in porous media actually measure the resistivity of the pore water, changes of which are directly related to porosity change. The sensor has been integrated in a measurement probe and a model pile to measure density changes continuously during penetration. This first implementation used in the geotechnical centrifuge shows the feasibility of the method, although the initial results also show some systematic errors resulting from the construction of the probe and the measurement method itself.

KEYWORDS: centrifuge modelling; laboratory equipment; piles; sands; soil/structure interaction

On a créé une sonde à résistivité électrique pour les essais sur modèle physique, afin d'examiner les variations de porosité survenant dans le sable de silice saturé. Pour des particules non conductrices, les mesures de résistivité électrique permettent de mesurer la résistivité de l'eau interstitielle, dont les variations sont en rapport direct avec les changements de porosité. Le capteur a été intégré dans une sonde de mesure et un modèle de pieu de façon à mesurer en continu les changements de densité survenant au cours de la pénétration. Cette première réalisation utilisée dans la centrifuge géotechnique démontre la faisabilité de cette méthode, même si les résultats initiaux fait état de certaines erreurs systématiques résultant de la structure de la sonde et de la méthode de mesure proprement dite.

INTRODUCTION

Measurements of soil density changes can be divided into optical methods and resistance methods. Optical methods include stereophotogrammetry (Davidson & Boghrat, 1983; De Pater & Nieuwenhuis, 1986), digital image correlation on natural soils (White, 2002; White & Bolton, 2004; Dijkstra *et al.*, 2006) or transparent soils (Hird & Stanier, 2010), X-ray measurements (Robinsky & Morrison, 1964; Kobayashi & Fukagawa, 2003) or other image processing techniques (Allersma, 1987). Resistance measurements have been performed on thermal resistance of the soil (Chong, 1988; Shublaq, 1992), as well as electrical resistance (Bezuijen & Mastbergen, 1989; Telford & Geldart, 1990). For soil density, or more precisely water content characterisation, nuclear probes (Ruygrok, 1977; Shibata *et al.*, 1992; Karthikeyan *et al.*, 2007) or electrical resistivity probes (Windle & Wroth, 1975; Vlasblom, 1977; Campanella & Weemees, 1990) are used. Electrical resistivity probes measure the apparent resistivity of the pore water that is correlated to the soil density using a linear relationship independent of grain shape (Archie, 1942; Jackson *et al.*, 1978). On the other hand nuclear probes use neutron scatter techniques to correlate radiation decay to water content.

With the exception of X-ray measurements or the use of transparent soils, the optical methods must be performed at a transparent boundary of the model container. This poses restraints on the possible failure modes that can be measured. Thermal and electrical probes are spatially less accurate, but allow deformations to develop around the probe, although they still could hamper the failure mechanism. A new smaller version of such a probe suitable for physical model tests will be presented in the current paper. Subsequently, the measured soil disturbance around such a probe during soil penetration is shown.

MEASUREMENT PRINCIPLE

In a resistivity measurement, the resistivity of the soil is measured, which according to Ohm's law is

$$\rho = \frac{AV}{IL} \tag{1}$$

with resistivity ρ, cross-sectional area A, voltage V, current I and length L. An idealised graphical presentation of equation (1) is given in Fig. 1. The geometrical properties, A and, L,

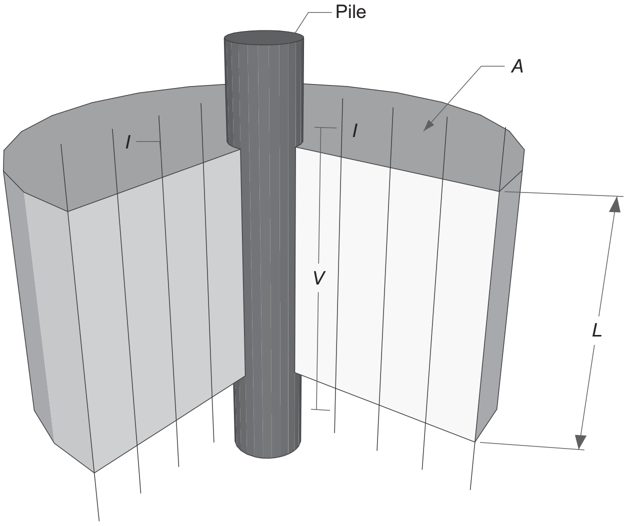

Fig. 1. Ohm's law around probe

Manuscript received 21 October 2008; revised manuscript accepted 7 October 2011. Published online ahead of print 7 June 2012.
Discussion on this paper closes on 1 January 2013, for further details see p. ii.

* Delft University of Technology, Geo-Engineering Section, Delft, The Netherlands.

are generally unknown if resistivity measurements of a body of soil are taken. If these properties are lumped into the calibration factor for the sensor, Ohm's law reduces to the well-known form

$$R = \frac{V}{I} \tag{2}$$

where R is resistance. It would be appropriate to name R the apparent resistance and ρ apparent resistivity, as the true resistivity is not measured. Actually, the apparent resistivity is the mean resistivity of the sand particles and the pore water. As pore water is a much better conductor, the resistivity is almost solely determined by the conductivity of the water and the amount of water in the pores. As a result, the resistivity measurement method can measure pore volume changes in saturated conditions, where any change in pore volume results in a change in pore water volume and subsequently in a change of the apparent resistivity.

For proper calibration of the measurement technique the size of the potential field, or the field of vision, should not change during penetration. In order to gain insight into the stability of this field of vision for different soil permittivities, the Maxwell equations have been solved for the current sensor design. The results in Fig. 2 show the potential field (V) in the soil at the level of the sensor as a function of the distance to the sensor.

Four cases are studied

- (*a*) a homogeneous medium dense, saturated sand layer
- (*b*) a fictive 15 mm thick zone of water directly next to the probe (effectively a short circuit), followed by medium dense sand
- (*c*) a 15 mm wide zone of dense sand next to the probe
- (*d*) a 15 mm wide zone of loose sand.

These calculations present a limiting state, therefore the loose state corresponds to the maximum porosity, $n_{\max}$, of the Baskarp sand, the dense state to the minimum value for the porosity, $n_{\min}$, and the medium dense has been chosen as a relative density of 50%. The field of vision, which defines the volume at which 50% of the charge is either inside or outside this volume, is also shown. The limited variation allows for the lumping of geometrical effects in a calibration factor and at the same time ascertains that any measured change in apparent resistivity is indicative of a density change near the probe. However, as the measurement method averages density change over its field of vision, local changes on a smaller scale cannot be distinguished.

Implementation

In the measurement probe, shown in Fig. 3, a potential field with constant current I is applied to the outer set of conductors vertically spaced at 10 mm. The inner set of conductors, spaced 3·3 mm apart, is used to measure the voltage drop V within this section of the potential field. All conductors are made of 1·5 mm thick stainless steel rings and are isolated from each other and the remainder of the probe. Combined, I and V yield the apparent resistivity. An electrical representation of the system is given in Fig. 4. The four conductors are represented as c_1–c_4. The current I is derived from the measurement of voltage V_c over a reference resistor R_{ref}, located in the power supply. The voltage drop in the soil V_s is measured over c_2 and c_3. It is assumed that the contact resistance between conductors and soil R_c is equal for all conductors. Regular checks of the contact resistance between the conductor and the connector did not show an appreciable change in contact resistance. The electrical isolation between the conductors was checked in a similar fashion; no internal short circuits were observed during the tests series.

The measurements are filtered with a 40 Hz Bessel low pass filter for suppression of the 50 Hz interference from the mains and sampled at 200 Hz using an HBM MgcPlus DAQ system with the HBM ML10B amplifier board. The soil apparent resistivity R_{soil} is derived from V_s and V_c by

$$R_{soil} = \frac{V_s R_{ref}}{V_c} \tag{3}$$

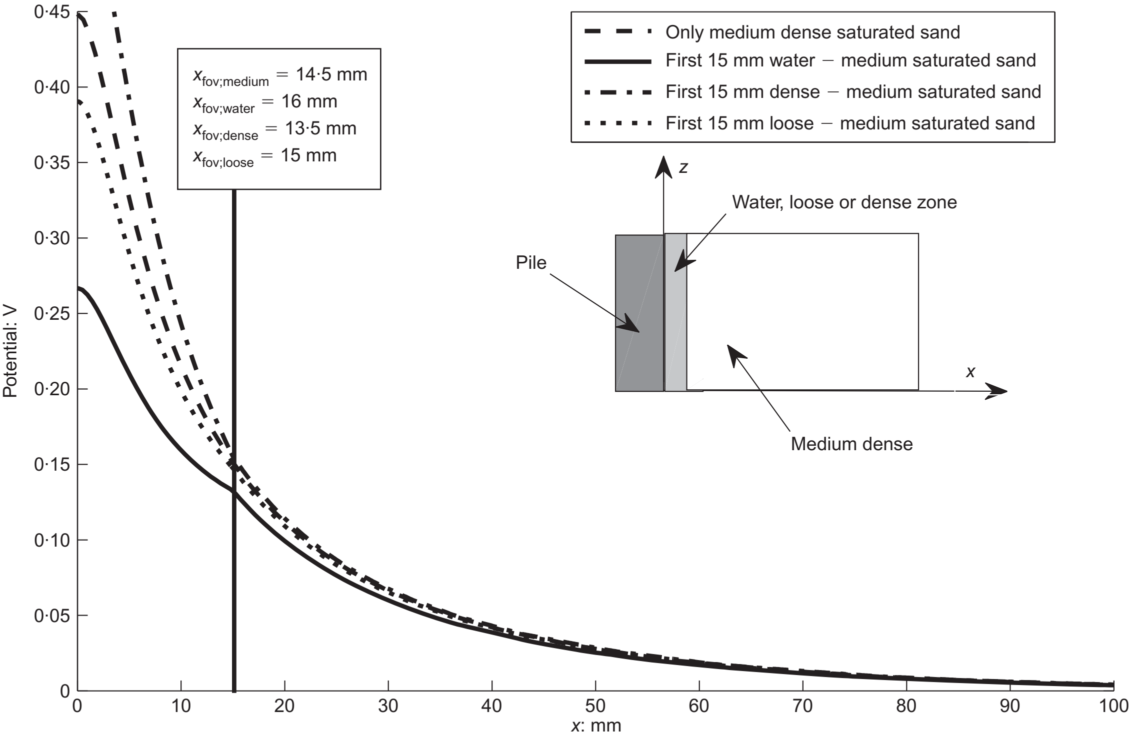

Fig. 2. Influence zone of measurement probe

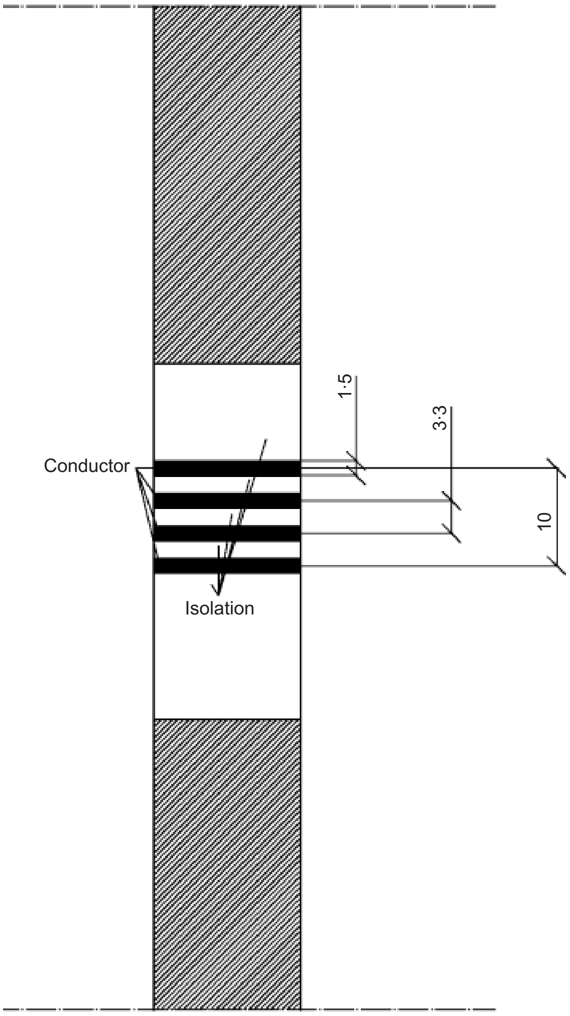

Fig. 3. Mechanical realisation of resistivity probe (measurements in mm)

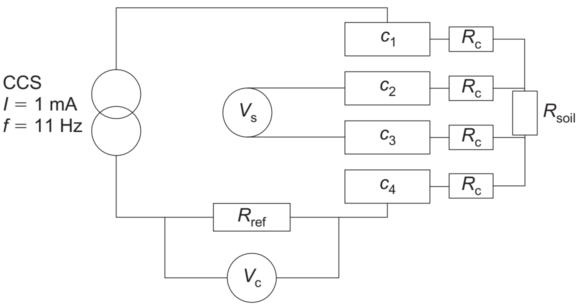

Fig. 4. Electrical circuit of resistivity measurement set-up; CCS is constant current source

To ensure stability of the power supply a high output impedance, 1 mA regulated current source modulated at 11 Hz is used. The modulation is obtained by feeding a solid-state relay with a periodic signal from a Hewlett Packard 3310B function generator.

Calibration

After assembly the prototype probe was calibrated in saturated Baskarp sand (properties in Table 1). De-aired tap water was used, in which approximately 1 g/l sodium chloride (NaCl) was dissolved in order to increase the conductivity of the water and thereby reducing the effects of electrode–soil contact impedance and internal losses in the probe. The sand was pumped in suspension from a storage vessel into the model container in which the probe was already fixed in place, and the sand was allowed to settle. The total amount of water in both the vessel and the model container is determined as accurately as possible for the amount of added sodium chloride, but mixing large quantities of water with the solute and estimating the amount of water in the storage vessel negatively impacted accuracy of the salinity preparation. The probe was initially embedded in the sand sample. A loose sample was obtained, with a porosity n of approximately 0·455. The sample could subsequently be densified by a vertical shock wave propagating through the sample and allowing simultaneous top and bottom drainage of the excess pore water (Van der Poel & Schenkeveld, 1998; Rietdijk *et al.*, 2010). In this way porosities up to $n = 0{\cdot}382$ were reached very consistently.

Table 1. Properties of Baskarp sand

Name	Symbol	Property
Saturated vol. weight: kN/m^3	γ_{sat}	18·7–20·9
Friction angle*	Φ_{cv}	34·5
Secant Young's modulus:* kN/m^2	E_{50}	6×10^3
Minimum porosity†	n_{min}	0·354
Maximum porosity†	n_{max}	0·481
Mean diameter: mm	d_{50}	0·135

* For 51 kPa effective stress and $n_c = 0{\cdot}408$.
† JGS (1990).

The calibrated sensitivity of two sensors is plotted in Fig. 5. The first probe has polyvinyl chloride (PVC) isolation between the conductors and forms part of an instrumented model pile, the second uses Nylon isolation rings between the conductors. During this calibration the sample was densified around the fixed probes. All sensors are calibrated at the same time in one sample. A linear trend between the porosity and the electrical resistivity is found, although at very dense soils the preparation method starts to be limiting. The difference in assembly results in a shifted and tilted response for each sensor.

Uncertainties in the measurement method

Differences in the observed sensitivity are due to system errors in the set-up. Uncertainties resulting from the preparation, however, lead to an absolute shift of the measured resistivity. These errors are introduced by the soil preparation method where the sodium chloride concentration of the water cannot be accurately controlled.

An absolute shift due to temperature changes on the apparent resistivity reading by a 1°C temperature change ΔT would change conductivity by 2% (Schoemaker *et al.*, 2007). Apart from the preparation related errors, the presented measurement method is also susceptible to a systematic error in the measured R_{soil}. This error can be derived from the error in the voltage readings δV_s and δV_c and the tolerance of the reference resistance δR_{ref}. Assuming a normal distribution of these errors it follows that

$$\delta R_{\mathrm{soil}} = \sqrt{\left|\frac{\partial R_{\mathrm{soil}}}{\partial V_s}\delta V_s\right|^2 + \left|\frac{\partial R_{\mathrm{soil}}}{\partial V_c}\delta V_c\right|^2 + \left|\frac{\partial R_{\mathrm{soil}}}{\partial R_{\mathrm{ref}}}\delta R_{\mathrm{ref}}\right|^2} \tag{4}$$

For the current set-up $\delta V_s = \delta V_c = 100$ μV. The tolerance of the reference resistor is 0·3%, including estimated mechanical (mainly solder joints) and temperature effects. This equates to a typical value for the systematic error of +/−0·5 Ω. The current sensing resistor was an ordinary metal film instead of

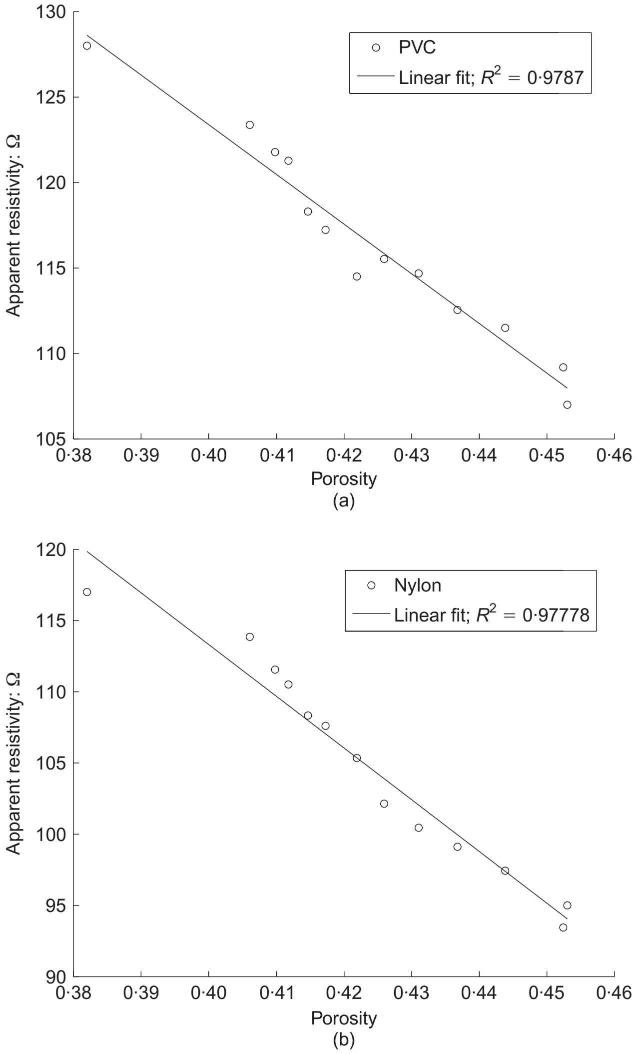

Fig. 5. Calibration of the resistivity sensors; 1 g/l sodium chloride added to the pore water: (a) PVC isolation between conductors; (b) nylon isolation between conductors

a precision film resistor (as with hindsight would have been required in these situations).

APPLICATIONS

Sensing soil densification resulting from centrifuge spin up

One of the possible uses for this probe is to sense the disturbance of very loose soil samples during centrifuge spin-up. Fig. 6 shows a typical result for the change in soil resistivity due to the change in r/min of the centrifuge. Note the difference in the absolute resistivity when compared to the calibration. This is due to the different conductivity of the pore water.

Normalised density change near a pile

In order to correct for the absolute shift in the resistivity due to uncertainties in the preparation when handling large models, the reading for the instrument level on the pile, R_{pile}, is adjusted by the first reading and subsequently adjusted with the stationary reference location, R_{ref}, before being converted to porosity change with the previously established slope resulting from the calibration.

$$\Delta n = c\left[\left(R_{\text{pile};i} - R_{\text{pile};0}\right) - \left(R_{\text{ref};i} - R_{\text{ref};0}\right)\right] \tag{5}$$

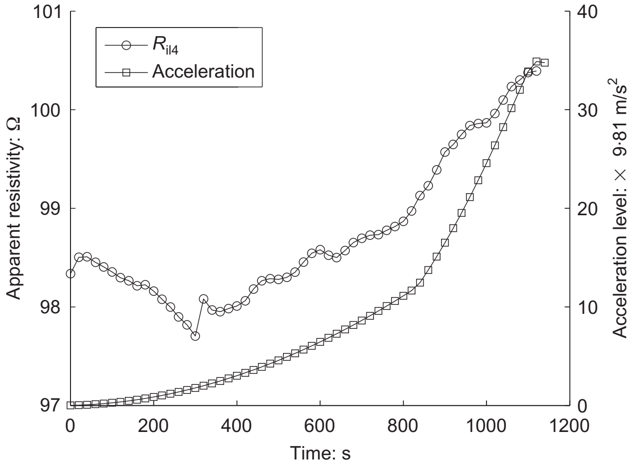

Fig. 6. Effect of centrifuge spin-up on apparent resistivity; initial porosity $n_0 = 0{\cdot}439$

In this way any absolute resistivity shift resulting from preparation or spin-up in the geotechnical centrifuge is mitigated. This shift converts all apparent resistivity measurements to readings of porosity change, and not absolute porosity. This normalisation leads to an increase of systematic error of +/−2 Ω.

As an example, the change in porosity in the soil adjacent to a displacement pile during installation is shown in Fig. 7. Five different tests have been performed in the geotechnical centrifuge of Deltares at 35***g***. The pile is installed at a model rate of 1 mm/s.

The results clearly show that one dense test ($n_0 = 0{\cdot}389$) and one medium dense test ($n_0 = 0{\cdot}414$) resulted in a distinctly different porosity change. All other tests show density changes of the same magnitude regardless of initial condition. A stationary state is reached after 5*D* pile displacement. The distinct peak at 2·3*D* corresponds to the instrument level exiting the pre-disturbed zone as the pile was pre-embedded.

CONCLUSIONS

A new method to investigate soil density change during pile installation based on electrical resistivity change is presented. The method proves to be sensitive to preparation conditions and subsequent experimental disturbances related to change in density of the sample, spin-up of the geotechnical centrifuge and variations in the salinity of the pore

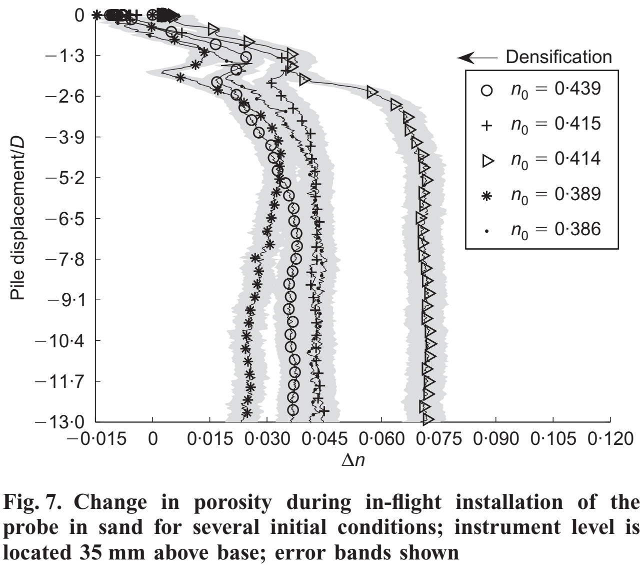

Fig. 7. Change in porosity during in-flight installation of the probe in sand for several initial conditions; instrument level is located 35 mm above base; error bands shown

water. The method shows promising results when used for capturing the soil density change near a model pile which is fully surrounded by soil.

ACKNOWLEDGEMENT

The technical and scientific staff of Deltares (formerly GeoDelft) are gratefully acknowledged for their help and expertise during the design and execution of the tests.

REFERENCES

Allersma, H. G. B. (1987). *Optical analysis of stress and strain in photoelastic particle assemblies*. PhD thesis, Delft University of Technology, The Netherlands.

Archie, G. E. (1942). The electrical resistivity log as an aid in determining some reservoir characteristics. *Trans. AIME* **146**, No. 5, 54–62.

Bezuijen, A. & Mastbergen, D. (1989). Liquefaction of a sand body constructed by means of hydraulic fill. *Proc. 12th Int. Conf. on Soil Mechanics and Foundation Engineering, Rio de Janeiro* **12**, 891–894.

Campanella, R. G. & Weemees, I. (1990). Development and use of an electrical resistivity cone for groundwater contamination studies. *Can. Geotech. J.* **27**, No. 5, 557–567.

Chong, M. K. (1988). Density changes of sand on cone penetration resistance. *Proc. 1st Int. Symposium on Penetration Testing ISOPT-1, Florida* **2**, 707–714.

Davidson, J. L. & Boghrat, A. (1983). Displacements and strains around probes in sand. *Proceedings of the conference on geotechnical practice in offshore engineering*, Austin, TX, USA (ed. S. G. Wright), pp. 181–202.

De Pater, C. J. & Nieuwenhuis, J. D. (1986). Method for measuring the deformations of a sand surface. *Géotechnique* **36**, No. 4, 581–585, http://dx.doi.org/10.1680/geot.1986.36.4.581.

Dijkstra, J., Broere, W. & Van Tol, A. F. (2006). Experimental investigation into the stress and strain development around a displacement pile. *Proc. 10th Int. Conf. Piling and Deep Found., Amsterdam* **10**, 252–259.

Hird, C. C. & Stanier, S. A. (2010). Modelling helical screw piles in clay using a transparent soil. *Proc. 7th Int. Conf. Phys. Modelling Geotech., Zurich* **2**, 769–774.

Jackson, P. D., Taylor Smith, D. & Stanford, P. N. (1978). Resistivity–porosity–particle shape relationshipis for marine sands. *Geophysics* **43**, No. 6, 1250–1268.

JGS (Japanese Geotechnical Society) (1990). *JGS 0161-1990: Soil testing standards. Test methods for the minimum and maximum densities of sands.* Tokyo, Japan: Japanese Geotechnical Society (in Japanese).

Karthikeyan, M., Tan, S. M., Mimura, M., Yoshimura, M., & Tee, C. P. (2007). Improvements in nuclear-density cone penetrometer for non-homogeneous soils. *Soils Found.* **47**, No. 1, 109–117.

Kobayashi, T. & Fukagawa, R. (2003). Characterization of deformation process of CPT using X-ray TV imaging technique. *Proc. 3rd Int. Conf. Deformation Characteristics Geomater.*, *IS-Lyon* **3**, 43–47.

Rietdijk, J., Schenkeveld, F. M., Schaminee, P. E. L. & Bezuijen, A. (2010). The drizzle method for sand sample preparation. *Proc. 7th Int. Conf. Phys. Modelling Geotechnics, Zurich*, 267–272.

Robinsky, E. I. & Morrison, C. F. (1964). Sand displacement and compaction around model friction piles. *Can. Geotech. J.* **1**, No. 2, 81–93.

Ruygrok, P. A. (1977). Electrical density measurements. *LGM-mededelingen* **18**, No. 2/3, 70–73.

Schoemaker, F. C., Smeulders, D. M. J. & Slob, E. C. (2007). Simultaneous determination of dynamic permeability and streaming potential. *SEG Expanded Abstr., RP 1 Lab Measmt* **26**, 1555–1559.

Shibata, T., Mimura, M., Shrivastava, A. K. & Nobuyama, M. (1992). Measurement by neutron moisture cone penetrometer: design and application. *Soils Found*. **32**, No. 4, 58–67.

Shublaq, J. (1992). Soil disturbance due to installation of model piles and pile groups. *Soils Found*. **32**, No. 4, 17–26.

Telford, W. & Geldart, L. (1990). *Applied geophysics*, 2nd edn. Cambridge, UK: Cambridge University Press.

Van der Poel, J. T. & Schenkeveld, F. M. (1998). A preparation technique for very homogeneous sand models and CPT research. *Proceedings of the international conference centrifuge 98*, Tokyo, Japan, pp. 149–154.

Vlasblom, A. (1977). Electrical density measurements. *LGM-mededelingen* **18**, No. 2/3, 69–70.

White, D. J. (2002). *An investigation into the behaviour of pressed-in piles*. PhD thesis, University of Cambridge, Cambridge, UK.

White, D. J. & Bolton, M. D. (2004). Displacement and strain paths during plane-strain model pile installation in sand. *Géotechnique* **54**, No. 6, 375–397, http://dx.doi.org/10.1680/geot.2004.54.6.375.

Windle, D. & Wroth, C. P. (1975). Electrical resistivity method for determining volume changes that occur during a pressuremeter test. *ASCE specialty conference on* in situ *measurement of soil properties*, Raleigh, NC, USA, pp. 497–510.